All-Optical Switching and Unidirectional Plasmon Launching with Nonlinear Dielectric Nanoantennas

Alex Krasnok,[1,2,*] Sergey Li,[2] Sergey Lepeshov,[2] Roman Savelev,[2] Denis G. Baranov,[3,4] and Andrea Alú[1,†]

[1]*The University of Texas at Austin, Austin, Texas 78712, USA*
[2]*Department of Nanophotonics and Metamaterials, ITMO University, St. Petersburg 197101, Russia*
[3]*Department of Physics, Chalmers University of Technology, 412 96 Gothenburg, Sweden*
[4]*Moscow Institute of Physics and Technology, Dolgoprudny 141700, Russia*

(Received 5 August 2017; revised manuscript received 4 November 2017; published 16 January 2018)

High-index dielectric nanoparticles have become a powerful platform for nonlinear nanophotonics due to special types of optical nonlinearity, e.g. caused by electron-hole plasma (EHP) photoexcitation. We propose a highly tunable dielectric nanoantenna consisting of a chain of silicon particles excited by a dipole emitter. The nanoantenna exhibits slow group-velocity guided modes, corresponding to the Van Hove singularity in an infinite structure, which enable a large Purcell factor up to several hundred and are very sensitive to the nanoparticle permittivity. This sensitivity enables the nanoantenna tuning via EHP excitation with an ultrafast laser pumping. Dramatic variations in the nanoantenna radiation patterns and Purcell factor caused by ultrafast laser pumping of several boundary nanoparticles with relatively low intensities of about 25 GW/cm^2 are shown. Unidirectional surface-plasmon polaritons launching with EHP excitation in the nanoantenna on a Ag substrate is demonstrated.

DOI: 10.1103/PhysRevApplied.9.014015

I. INTRODUCTION

In the last several years, dielectric nanoparticles and nanostructures made of materials with large positive dielectric permittivity, such as Si, GaP, and GaAs, have proved to be a promising platform for various nanophotonic applications [1–3]. The examples include functional nanoantennas [4–6], enhanced spontaneous emission [7–11], photovoltaics [12], frequency conversion [13–16], Raman scattering [17], and sensing [7,18]. The great interest in such nanostructures is caused mainly by their ability to control the electric and magnetic components of light at the nanoscale, as well as low dissipative loses and thermal heating [18]. For example, it has been demonstrated that dielectric nanoantennas allow directional scattering of an incident light and effective transformation of the near field of feeding quantum emitters (QEs) into propagating electromagnetic waves [3,7].

Modification of the spontaneous emission rate of a QE induced by its environment, known as the Purcell effect [19,20], is not so pronounced for single dielectric nanoparticles [3,21], in contrast to microcavities [22] and plasmonic nanoantennas [23,24]. This is the case because of their relatively low quality factors and large mode volumes, which result in the low efficiency of the light-matter interaction. However, it was recently shown that this obstacle can be overcome by relying on slowly guided modes in chain nanostructures. It turns out that the Purcell factor can be increased by several orders of magnitude in finite chains of Si nanoparticles [25]. The role of Van Hove singularities associated with infinite structures in the high-Purcell-factor enhancement has been revealed by using an eigenmode analysis. Moreover, the collective nature of these modes makes the structure very sensitive to any changes in geometry, opening the way to the creation of highly tunable devices.

High-index dielectric nanostructures attract special interest for nonlinear nanophotonics because of their strong nonlinear response. It was recently predicted and experimentally demonstrated that photoexcitation of dense electron-hole plasma (EHP) in single Si nanoparticles [26–28] and Si nanodimers [29] by femtosecond laser pulses is accompanied by a modification of the radiation properties, whereas the generation of EHP in Ge nanoantennas can even turn them into plasmonic ones in the mid-IR region [30]. In this regard, we note that, in contrast to metals, whose conduction band is already partially filled at room temperature, the conduction band of semiconductors is almost empty and the generation of EHP may significantly modify their plasma frequency and dielectric permittivity [28].

Here, we combine the concepts of Van Hove singularity and EHP excitation together and propose a highly tunable dielectric nanoantenna, consisting of a Si nanoparticle chain excited by an electric dipole emitter. The nanoantenna possess slowly guided modes corresponding to the Van Hove singularity in an infinite chain. Since these modes are

*akrasnok@utexas.edu
†alu@mail.utexas.edu

very sensitive to the nanoparticle permittivity, the radiation properties of the nanoantenna become extremely sensitive to EHP photoexcitation. We theoretically and numerically demonstrate the tuning of the radiation power patterns and the Purcell factor by pumping several boundary nanoparticles in the chain with relatively low peak intensities of femtosecond laser pulses. Moreover, we show that the proposed nanoantenna, being excited by femtosecond laser pulses, allows unidirectional launching of surface-plasmon-polariton (SPP) waves (Fig. 1), making this solution attractive for all-optical light-manipulation systems. We note that, in contrast to the established approaches to unidirectional SPP wave excitation [31–35], nonlinear waveguiding systems with QEs as a source are still weakly developed, although they may have many important applications in nanophotonics and quantum optics.

II. RESULTS AND DISCUSSION

To briefly recall the origin of the *Van Hove singularity*, let us consider a generic periodic one-dimensional system supporting a set of guided modes. Decomposing its Green's tensor into a series of eigenmodes, one can calculate the Purcell factor in such a system according to Ref. [36],

$$F \simeq \frac{1}{\pi}\left(\frac{\lambda}{2}\right)^2 \frac{c}{A_{\mathrm{eff}} V_{\mathrm{gr}}}, \tag{1}$$

with A_{eff} being the effective area of the resonant guided mode, λ the free-space wavelength, V_{gr} the group velocity of the mode, and c the speed of light. The divergence of the Purcell factor, occurring at the point of zero group velocity, is known as a Van Hove singularity. This expression clearly suggests that the Purcell factor benefits from slow-light modes of the structure. In reality, its finite size prevents this divergence, but, nevertheless, a largely enhanced Purcell factor can still be traced to the Van Hove singularity of the original structure, as was theoretically and experimentally shown in Ref. [25].

In Fig. 1, we realize a Van Hove singularity using a chain of N spherical dielectric nanoparticles excited by an electric dipole (the green arrow), placed in the center of the chain and perpendicularly oriented to the chain axis. We choose Si particles with a dielectric permittivity ε_1 close to 16 in the operational frequency range [37]. The nanoparticles all have the same radius r, and the center-to-center distance between neighboring particles is a.

The optical properties of nanoparticle-based nanoantennas can be understood from the infinite-chain modal dispersion [38,39]. Therefore, we start by calculating the optical properties of the infinite structure with an analytical approach, based on the well-known coupled-dipole model. Each particle is modeled as a combination of magnetic and electric dipoles with magnetic $\mathbf{m}$ and electric $\mathbf{p}$ momenta, oscillating with frequency ω [$\propto \exp(-i\omega t)$].

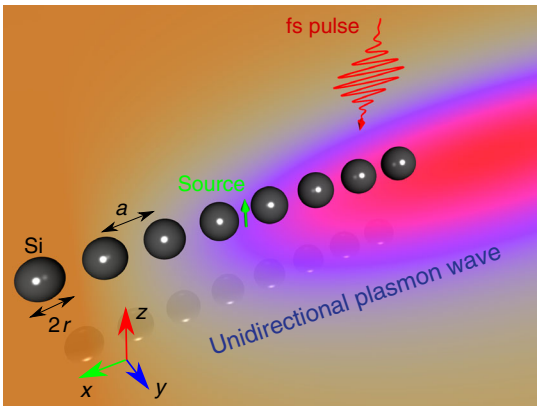

FIG. 1. Schematic presentation of a nonlinear dielectric nanoantenna tunable with electron-hole plasma photoexcitation via femtosecond-laser-pulse pumping of a few boundary nanoparticles. The nanoantenna allows us to tune the Purcell factor and radiation power pattern of a QE (the green arrow), and enables the unidirectional launching of propagating plasmonic surface waves.

In the centimeter-gram-second system, this approach leads to the linear system of equations

$$\begin{aligned}\mathbf{p}_i &= \alpha_{ei}\sum_{j\neq i}(\hat{C}_{ij}\mathbf{p}_j - \hat{G}_{ij}\mathbf{m}_j),\\ \mathbf{m}_i &= \alpha_{mi}\sum_{j\neq i}(\hat{C}_{ij}\mathbf{m}_j + \hat{G}_{ij}\mathbf{p}_j),\end{aligned} \tag{2}$$

where $\hat{C}_{ij} = A_{ij}\hat{I} + B_{ij}(\hat{\mathbf{r}}_{ij}\otimes\hat{\mathbf{r}}_{ij})$, $\hat{G}_{ij} = -D_{ij}\hat{\mathbf{r}}_{ij}\times\hat{I}$, $\otimes$ is the dyadic product, $\hat{I}$ is the unit 3×3 tensor, $\hat{\mathbf{r}}_{ij}$ is the unit vector in the direction from the ith to the jth sphere, and

$$\begin{aligned}A_{ij} &= \frac{\exp(ik_h r_{ij})}{r_{ij}}\left(k_h^2 - \frac{1}{r_{ij}^2} + \frac{ik_h}{r_{ij}}\right),\\ B_{ij} &= \frac{\exp(ik_h r_{ij})}{r_{ij}}\left(-k_h^2 + \frac{3}{r_{ij}^2} - \frac{3ik_h}{r_{ij}}\right),\\ D_{ij} &= \frac{\exp(ik_h r_{ij})}{r_{ij}}\left(k_h^2 + \frac{ik_h}{r_{ij}}\right),\end{aligned} \tag{3}$$

where r_{ij} is the distance between the centers the of ith and jth spheres, ε_h is the permittivity of the host medium, $k_h = \sqrt{\varepsilon_h}\omega/c$ is the host wave number, $\omega = 2\pi\nu$, and ν is the frequency. The quantities α_m and α_e are the magnetic and electric polarizabilities of a spherical particle [40]:

$$\alpha_e = i\frac{3\varepsilon_h a_1}{2k_h^3}, \qquad \alpha_m = i\frac{3b_1}{2k_h^3}, \tag{4}$$

where a_1 and b_1 are electric and magnetic Mie coefficients. The coupled-dipole approximation outlined above is justified for the geometrical parameters of the nanoparticles and their relative distance [41].

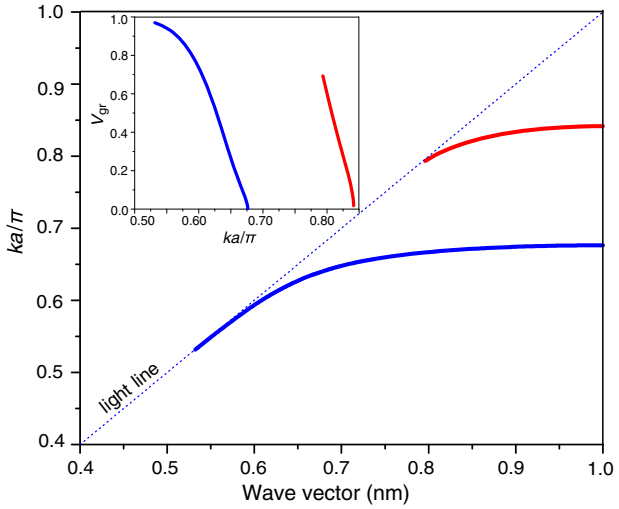

FIG. 2. Dispersion diagram of an infinite chain of dielectric nanoparticles with radius $r = 70$ nm and period $a = 200$ nm. (Inset) Group velocity (V_{gr}) of waveguiding modes in the infinite chain as a function of normalized frequency. The blue and red curves correspond to TM and TE modes, respectively.

The solution of Eq. (2) without a source [dispersion of waveguide eigenmodes $\omega(k)$] for the infinite dielectric chain with $r = 70$ nm and $a = 200$ nm in free space is shown in Fig. 2. Here, we use the dimensionless wave number $q = \beta a/\pi$, where β is the Bloch propagation constant. For simplicity but without loss of generality, we model silicon on a material with permittivity of 16 at a wavelength of 600 nm, which is close to the experimental data [37]. The blue and red curves correspond to transverse-magnetic (TM) and transverse-electric (TE) modes, respectively, which are the only modes excited by the dipole QE with the chosen orientation. Both of these modes are characterized by induced magnetic and electric moments (except the points at the band edge). Because of the spectral separation of resonances of the single particle, the magnetic moments are dominant in the first branch (TM), and electric moments in the second one (TE). The inset in Fig. 2 shows the calculated group velocities of the waveguide modes as a function of frequency. It can be seen that the group velocity V_{gr} drops to zero at the band edge around $ka/\pi \approx 0.675$ and $ka/\pi \approx 0.83$. Since the symmetry of the electric dipole source matches the symmetry of the TM staggered mode (but not the TE one), we may expect significant enhancement of the Purcell factor for a finite system around $ka/\pi \approx 0.675$.

To confirm this expectation, we calculate the Purcell factor using the Green's tensor approach [42]:

$$F = \frac{3}{2k_h^3}\mathbf{z}\cdot \mathrm{Im}[\mathbf{G}(0,0;\omega)]\cdot \mathbf{z}, \tag{5}$$

with $\mathbf{G}(0,0;\omega)$ being the Green's tensor of an electric dipole in the center of a chain (the point of the dipole QE localization) and $\mathbf{z}$ being the unit vector pointing in the z direction (Fig. 1). Practically, the quantity $\mathrm{Im}[\mathbf{G}(0,0;\omega)]$ can be found by solving the scattering problem with the dipolar QE outlined above, Eqs. (2)–(4).

Figure 3 shows the calculated Purcell factor as a function of wavelength and ratio r/a for a QE located in the center of a dielectric chain with different numbers of particles: (a) $N = 4$, (b) $N = 6$, (c) $N = 8$, and (d) $N = 10$. We observe that increasing the number of nanoparticles N gives rise to an enhancement of the Purcell factor. For example, the maximal value of the Purcell factor for $N = 10$ reaches 250. Along with the calculations shown in Fig. 2, we

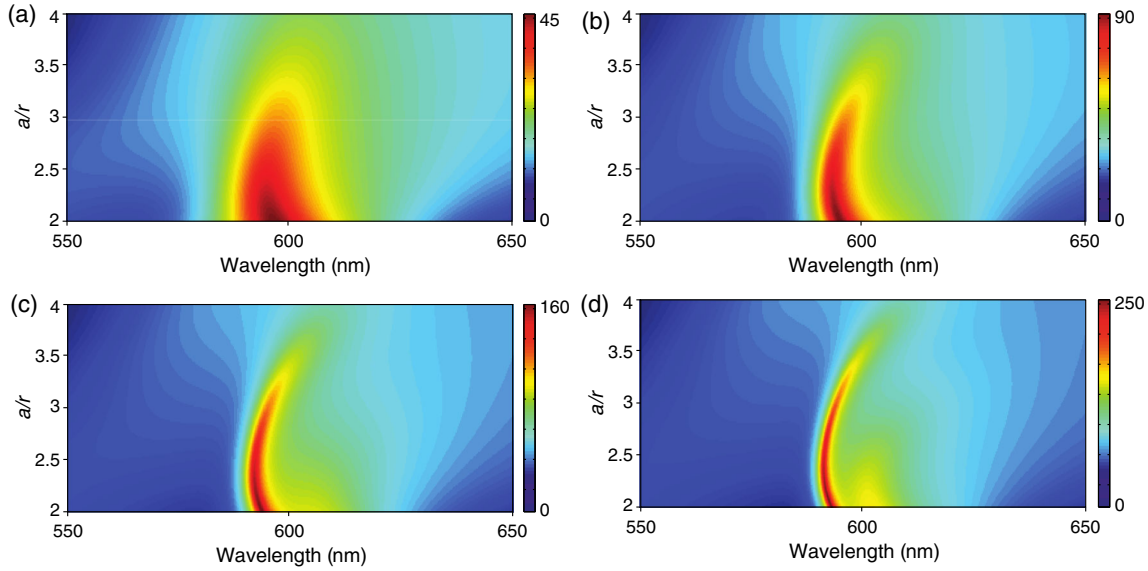

FIG. 3. Log-scale Purcell factor as the function of the radiation wavelength and ratio r/a for a dielectric chain with $\varepsilon_1 = 16$, for different number of nanoparticles: (a) $N = 4$, (b) $N = 6$, (c) $N = 8$, and (d) $N = 10$; r is set at 70 nm, a is a period of the chain.

conclude that the maximum of the Purcell factor arises around the Van Hove singularity.

Next, we show that the excitation of slow guided modes determining a Van Hove singularity is very sensitive to the electrodynamic properties of the system. Our aim is to utilize this effect to engineer highly tunable nanoantennas, for which relatively low intensities of external laser pulses can control and cause a dramatic modification of the optical properties of the material, and consequently the radiation properties (the intensities of emission and power patterns) of the nanoantenna. To enable the switching of the nanoantenna properties, we employ the nonlinear response caused by *electron-hole plasma photoexcitation* the in boundary particles of the Si nanoantenna.

To describe EHP-induced tuning of the nanoantenna, we employ the analytical approach developed in Ref. [28]. The dynamics of volume-averaged EHP density ρ_{eh} is modeled via the rate equation

$$\frac{d\rho_{\mathrm{eh}}}{dt} = -\Gamma\rho_{\mathrm{eh}} + \frac{W_1}{\hbar\omega} + \frac{W_2}{2\hbar\omega}, \tag{6}$$

where $W_{1,2}$ represents the volume-averaged absorption rates due to one- and two-photon processes, and Γ is the EHP recombination rate that depends on the EHP density [43]. The absorption rates are written in the usual form as $W_1 = [\omega/(8\pi)]\langle|\tilde{\mathbf{E}}_{\mathrm{in}}|^2\rangle \mathrm{Im}(\varepsilon)$ and $W_2 = [\omega/(8\pi)]\langle|\tilde{\mathbf{E}}_{\mathrm{in}}|^4\rangle \mathrm{Im}\chi^{(3)}$, where the angle brackets denote averaging over the nanoparticle volume, and $\mathrm{Im}\chi^{(3)} = [(\varepsilon c^2)/8\pi\omega]\beta_{\mathrm{TPA}}$, with β_{TPA} being the two-photon-absorption coefficient. The relaxation rate of EHP in c-Si is dominated by Auger recombination $\Gamma = \Gamma_A\rho_{\mathrm{eh}}^2$ with $\Gamma_A = 4\times10^{-31}$ s^{-1} cm^6 [44].

Equation (6) describes the volume-averaged concentration of EHP $\rho_{\mathrm{eh}}(t)$, neglecting its spatial distribution and, hence, diffusion of carriers across the particle volume. At $\rho_{\mathrm{eh}} > 10^{20}$ cm^{-3}, the thermal velocity of the hot free electrons is about $v \approx 5\times10^5$ cm/s [45], whereas the corresponding electron-electron scattering time is about 100 fs. The characteristic EHP homogenization time governed by a ballistic motion of electrons can therefore be estimated as $\tau_{\mathrm{hom}} \approx r/2v \approx 100$ fs, where r is the nanoparticle radius. As one can see, the estimated diffusion time is much smaller than the EHP recombination time and is comparable to the incident-pulse duration.

The permittivity of photoexcited Si should be related to the time-dependent EHP density:

$$\varepsilon(\omega,\rho_{\mathrm{eh}}) = \varepsilon_0 + \Delta\varepsilon_{\mathrm{bgr}} + \Delta\varepsilon_{\mathrm{bf}} + \Delta\varepsilon_D, \tag{7}$$

where ε_0 is the permittivity of the nonexcited material, while $\Delta\varepsilon_{\mathrm{bgr}}$, $\Delta\varepsilon_{\mathrm{bf}}$, and $\Delta\varepsilon_D$ are the contributions from band-gap renormalization, band filling, and the Drude term, respectively. The detailed expressions for all contributions in Eq. (7) can be found in Ref. [28]. In total, these three contributions lead to a decrease of the real part of the permittivity with an increasing EHP density.

The spectral dependency of the Purcell factor before and after EHP photoexcitation is presented in Fig. 4 for different numbers of particles N. The calculations are performed for the change of the real part of Si permittivity $\Delta\varepsilon = -1$ [where $\Delta\varepsilon = \varepsilon(\omega,\rho_{\mathrm{eh}}) - \varepsilon_0$], which is achieved at a wavelength of 600 nm upon excitation of the EHP with density $\rho_{eh} \approx 10^{21}$ cm^{-3}. The decrease of the Purcell factor by approximately a factor of 2 in all cases [Figs. 4(a), 4(c), and 4(e)], along with the spectral broadening, is caused by symmetry breaking of the chain and a corresponding decrease of the quality factor of the Van Hove singularity mode. The EHP photoexcitation also modifies the radiation pattern of the nanoantenna [Figs. 4(b), 4(d), and 4(f)]. Before the plasma excitation ($\Delta\varepsilon = 0$), the radiation pattern exhibits two symmetric lobes directed along the chain axis in the forward and backward directions (the red curves). In this case, the maximal value of directivity grows with an increase in N. After the plasma excitation ($\Delta\varepsilon = -1$), the nanoantenna radiates mostly in the direction of the affected particles. We note that the degree of modification of the radiation pattern grows with an increasing number of particles. For example, in the case of $N = 8$ [Fig. 4(f)], the

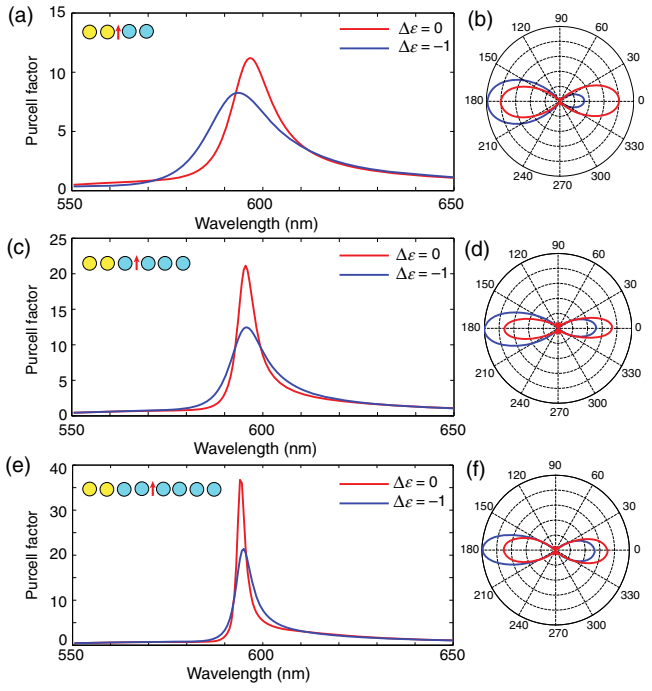

FIG. 4. (a),(c),(e) Spectral dependence of the Purcell factor for the chains of dielectric nanoparticles ($r = 70$ nm) for different numbers of nanoparticles N: (a) $N = 4$, (c) $N = 6$, and (e) $N = 8$. (b),(d),(f) Radiation power patterns (the E plane) of the QE at a radiation wavelength of 600 nm for different numbers of nanoparticles N. The red curves correspond to the unaffected chains ($\Delta\varepsilon = 0$), whereas the blue ones correspond to the chains with photoexcited boundary particles ($\Delta\varepsilon = -1$).

directivity in the left direction is almost 2 times larger than that in the right direction. Thus, the EHP photoexcitation can be applied to the all-optical switching of radiation patterns. Such dramatic tuning of the radiation pattern is caused by the Van Hove singularity regime of the initially unaffected nanoantenna. We notice that the proposed nanoantenna exhibits a QE position tolerance of about 30 nm [46], which is enough for practical realization with existing technologies of quantum-dot positioning [47].

In the vast majority of nanoantenna realizations, the substrate substantially affects the nanoantenna characteristics (see, for example, Ref. [48]). For this reason, we analyze how a SiO_2 substrate affects the nanoantenna's characteristics. To simulate a nanoantenna consisting of eight nanoparticles, located on the SiO_2 substrate with $\varepsilon_{sub} = 2.21$, we utilize the commercial software CST Microwave Studio. To calculate the Purcell factor, the method based on the input impedance of a small (in terms of radiation wavelength) dipole antenna [49] is applied. The corresponding results are presented in Fig. 5(a). These spectra qualitatively agree with the analytical calculations presented above. However, in this case, the substrate breaks the mirror symmetry with respect to the z axis, which leads to a reduction in the Purcell factor. From the experimental

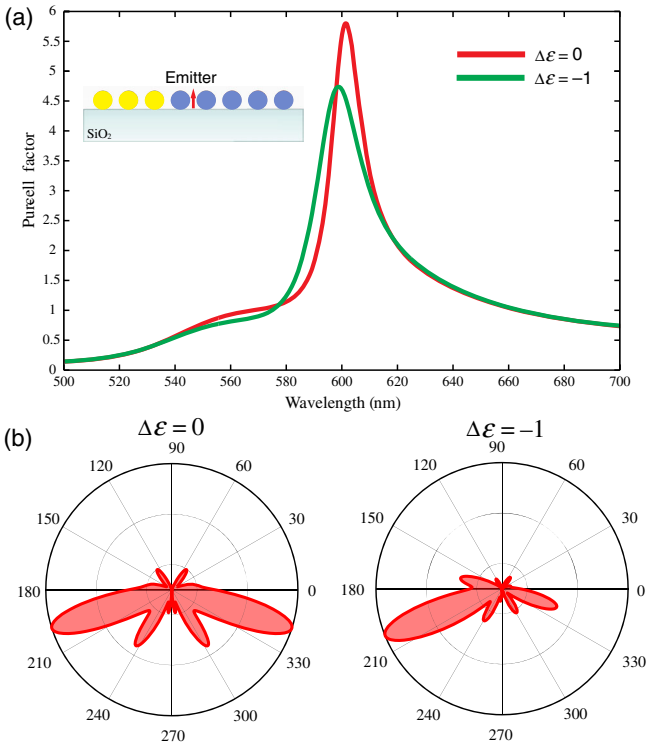

FIG. 5. (a) Purcell factor for a chain of $N = 8$ Si spherical particles ($r = 70$ nm) arranged on a SiO_2 substrate as a function of radiation wavelength. The difference between the dielectric permittivity of an unaffected and three left-boundary-affected particles is $\Delta\varepsilon = 0$ (the red curve) and $\Delta\varepsilon = -1$ (the green curve). (b) Power patterns for different values of $\Delta\varepsilon$.

standpoint, a laser pulse can be tightly focused to a subwavelength spot by an oil-immersion microscope objective with a large numerical aperture (NA). For example, an objective with NA = 1.4 can provide the full-width-at-half-maximum diameter of the beam focal spot size of $d = 560$ nm at a wavelength of 650 nm, according to the relation $d \approx 1.22\lambda/\mathrm{NA}$ [50,51]. This spot size corresponds to three boundary nanoparticles that are assumed to be affected [see the inset in Fig. 5(a)]. During the EHP photoexcitation, the maximum of the Purcell factor slightly decreases from 5.9 to 4.7, accompanied by a shifting of the resonant frequency to shorter wavelengths due to a decrease of the boundary particles' dielectric permittivity.

Figure 5(b) demonstrates the change in radiation pattern induced by EHP photoexcitation for the nanoantenna on a SiO_2 substrate. When $\Delta\varepsilon = 0$ (the unaffected nanoantenna), the radiation power pattern is symmetric with respect to the dipole axis and has two main lobes. It can be observed that the mirror symmetry of the radiation patterns with respect to the z axis is broken, and the main lobes are oriented into the substrate, which has a higher refractive index than the upper space. The modification of the three boundary particles dramatically changes the power pattern: the reconfiguration is sufficient for practical applications even when $\Delta\varepsilon = -1$.

This effect can be used for the unidirectional launching of waveguide modes in plasmonic waveguides at will. Figure 6 demonstrates this phenomenon, showing the calculated radiation of a nanoantenna composed of eight Si nanoparticles placed with the period of 200 nm on a silver substrate with the 60-nm spacer glass (SiO_2) layer. The SiO_2 spacer serves as a buffer layer for the protection of silver substrate from sulfidation. The QE is located at the center of the chain, perpendicular to the substrate. Figures 6(a) and 6(b) show the electric-field-distribution profile and the electric-field intensity, respectively, as a function of the x coordinate in cases with an unaffected nanoantenna. It can be seen that the nanoantenna launches surface plasmons symmetrically to the positive and negative directions of axis x. However, when three boundary nanoparticles are illuminated by the pump beam, the nanoantenna launches surface plasmons almost unidirectionally [Figs. 6(c) and 6(d)]. We achieve a front-to-back ratio of up to 5 for this geometry [Fig. 6(d)]. The plots in Figs. 6(b) and 6(c) exhibit two types of oscillation: in the vicinity of the nanoantenna and apart from it. The first type is caused by field localization around Si nanoparticles due to their resonant response. The second is due to a small reflection from open boundaries in the simulation region. This reflection is caused by the Ag substrate with real losses and dispersion.

We note that the methods to create the proposed nanoantenna do exist. Namely, in Ref. [52], the method to assemble colloidal nanoparticles of different natures

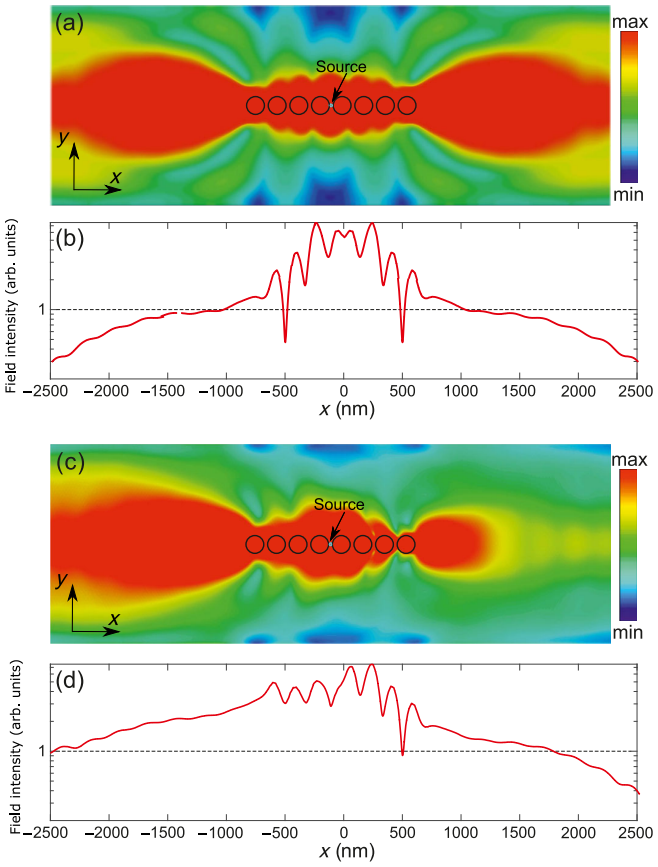

FIG. 6. Radiation of the nanoantenna composed by eight Si spherical particles ($r = 70$ nm) placed with a period of 200 nm on a Ag substrate with a 60-nm spacer glass layer; a QE is located at the center of the chain, perpendicular to the substrate. (a),(c) Electric-field-distribution profiles in the plane orthogonal to the QE in the cases of unaffected $\Delta\varepsilon = 0$ and affected $\Delta\varepsilon = -1$ three left boundary nanoparticles, respectively. (b),(d) Electric field intensities as a function of x coordinate in the cases of unaffected and affected three boundary nanoparticles, respectively. The emission wavelength is 600 nm.

(dielectric, metallic, and polymeric) was proposed. It has been demonstrated that structures of any complexity and composition can be created from sub-500-nm nanoparticles under a light-controlled temperature field. We believe that this approach can be applied directly to our nanoantenna fabrication. We note that the proposed approach to the nonlinear nanoantenna design also works for nanoantennas composed of cylindrical nanoparticles [53], which can be fabricated with existing lithography-based methods.

As the next step of our analysis, we estimate the parameters of the pump pulse required for the generation of 10^{21} cm^{-3} EHP, which is assumed in the electromagnetic calculations above. At the high intensities required for the photoexcitation of Si, two-photon absorption (TPA) usually dominates over the one-photon process [28]. Silicon has a particularly large TPA coefficient at wavelengths between 600 and 700 nm [54]. We set the wavelength of the pump pulse to 650 nm in order to avoid interference between the pump and the QE signals. Estimating the enhancement factors for $\langle|\tilde{\mathbf{E}}_{\mathrm{in}}|^2\rangle$ and $\langle|\tilde{\mathbf{E}}_{\mathrm{in}}|^4\rangle$ for a Si nanoparticle on a substrate and using Eq. (6) to calculate the dynamics of EHP density, we find that a 200-fs pulse with peak intensity of 25 GW/cm^2 provides 10^{21} cm^{-3} EHP in the nanoparticle on a silver substrate. The EHP relaxation time at such a density is about 2 to 3 ps, as was reported in Refs. [28,29], which should be sufficient for an ultrafast modulation of the emission process of a typical emitter with a lifetime in the nanosecond range.

Finally, we stress that an intensity of approximately 25 GW/cm^2 is much weaker than typical values of damage threshold for metallic and dielectric nanostructures. For example, gold nanorods have a damage threshold of about 70 GW/cm^2 or approximately 10 mJ/cm^2 at 130 fs [55], gold G-shaped nanostructures roughly 100 GW/cm^2 or about 3 mJ/cm^2 at 30 fs [56], and gold nanocylinders approximately 200 GW/cm^2 or about 20 mJ/cm^2 at 100 fs [57]. According to known data from the literature, low-loss silicon nanoparticles have significantly higher damage thresholds: roughly 400 GW/cm^2 or about 100 mJ/cm^2 at 250 fs [58], and approximately 1000 GW/cm^2 or about 100 mJ/cm^2 at 100 fs [26].

III. CONCLUSIONS

In this paper, we propose a highly tunable all-dielectric nanoantenna, consisting of a chain of Si nanoparticles excited by a quantum emitter, that allows their radiation properties to be tuned via electron-hole plasma photoexcitation. We theoretically and numerically demonstrate the tuning of radiation power patterns and the Purcell effect by the additional pumping of several boundary nanoparticles with relatively low peak intensities. We also demonstrate that these effects remain valid for the nanoantenna situated on a dielectric surface. The proposed nanoantenna allows for the tunable unidirectional launching of surface-plasmon waves, with interesting implications for modern nonlinear nanophotonics.

ACKNOWLEDGMENTS

This work was financially supported by the Russian Science Foundation (Grant No. 17-19-01731) and by the Russian Foundation for Basic Research (Project No. 16-37-60076). This work was also partially supported by the U.S. Air Force Office of Scientific Research with Grant No. FA9550-17-1-0002.

[1] Arseniy I. Kuznetsov, Andrey E. Miroshnichenko, Mark L. Brongersma, Yuri S. Kivshar, and Boris Luk'yanchuk,

Optically resonant dielectric nanostructures, Science **354**, aag2472 (2016).
[2] Saman Jahani and Zubin Jacob, All-dielectric metamaterials, Nat. Nanotechnol. **11**, 23 (2016).
[3] Alexander E. Krasnok, Andrey E. Miroshnichenko, Pavel A. Belov, and Yuri S. Kivshar, All-dielectric optical nanoantennas, Opt. Express **20**, 20599 (2012).
[4] Brice Rolly, Jean-Michel Geffrin, Redha Abdeddaim, Brian Stout, and Nicolas Bonod, Controllable emission of a dipolar source coupled with a magneto-dielectric resonant subwavelength scatterer, Sci. Rep. **3**, 3063 (2013).
[5] Alexander E. Krasnok, Constantin R. Simovski, Pavel A. Belov, and Yuri S. Kivshar, Superdirective dielectric nanoantennas, Nanoscale **6**, 7354 (2014).
[6] Sergey V. Li, Denis G. Baranov, Alexander E. Krasnok, and Pavel A. Belov, All-dielectric nanoantennas for unidirectional excitation of electromagnetic guided modes, Appl. Phys. Lett. **107**, 171101 (2015).
[7] Alex Krasnok, Martin Caldarola, Nicolas Bonod, and Andrea Alú, Spectroscopy and biosensing with optically resonant dielectric nanostructures, Adv. Opt. Mater. (2018).
[8] Raju Regmi, Johann Berthelot, Pamina M. Winkler, Mathieu Mivelle, Julien Proust, Frédéric Bedu, Igor Ozerov, Thomas Begou, Julien Lumeau, Hervé Rigneault, María F. García-Parajó, Sébastien Bidault, Jérôme Wenger, and Nicolas Bonod, All-dielectric silicon nanogap antennas to enhance the fluorescence of single molecules, Nano Lett. **16**, 5143 (2016).
[9] Dorian Bouchet, Mathieu Mivelle, Julien Proust, Bruno Gallas, Igor Ozerov, Maria F. Garcia-Parajo, Angelo Gulinatti, Ivan Rech, Yannick De Wilde, Nicolas Bonod, Valentina Krachmalnicoff, and Sébastien Bidault, Enhancement and Inhibition of Spontaneous Photon Emission by Resonant Silicon Nanoantennas, Phys. Rev. Applied **6**, 064016 (2016).
[10] S. Sun, L. Wu, P. Bai, and C. E. Png, Fluorescence enhancement in visible light: Dielectric or noble metal?, Phys. Chem. Chem. Phys. **18**, 19324 (2016).
[11] Alexander E. Krasnok, Alex Maloshtan, Dmitry N. Chigrin, Yuri S. Kivshar, and Pavel A. Belov, Enhanced emission extraction and selective excitation of NV centers with all-dielectric nanoantennas, Laser Photonics Rev. **9**, 385 (2015).
[12] Mark L. Brongersma, Yi Cui, and Shanhui Fan, Light management for photovoltaics using high-index nanostructures, Nat. Mater. **13**, 451 (2014).
[13] Alexander Krasnok, Mykhailo Tymchenko, and Andrea Alù, Nonlinear metasurfaces: A paradigm shift in nonlinear optics, Mater. Today (Oxford), DOI: 10.1016/j.mattod.2017.06.007 (2017).
[14] L. Carletti, A. Locatelli, O. Stepanenko, G. Leo, and C. De Angelis, Enhanced second-harmonic generation from magnetic resonance in AlGaAs nanoantennas, Opt. Express **23**, 26544 (2015).
[15] S. V. Makarov, A. N. Tsypkin, T. A. Voytova, V. A. Milichko, I. S. Mukhin, A. V. Yulin, S. E. Putilin, M. A. Baranov, A. E. Krasnok, I. A. Morozov *et al.*, Self-adjusted all-dielectric metasurfaces for deep ultraviolet femtosecond pulse generation, Nanoscale **8**, 17809 (2016).
[16] Alexander S. Shorokhov, Elizaveta V. Melik-Gaykazyan, Daria A. Smirnova, Ben Hopkins, Katie E. Chong, Duk-Yong Choi, Maxim R. Shcherbakov, Andrey E. Miroshnichenko, Dragomir N. Neshev, Andrey A. Fedyanin, and Yuri S. Kivshar, Multifold enhancement of third-harmonic generation in dielectric nanoparticles driven by magnetic Fano resonances, Nano Lett. **16**, 4857 (2016).
[17] Pavel A. Dmitriev, Denis G. Baranov, Valentin A. Milichko, Sergey V. Makarov, Ivan S. Mukhin, Anton K. Samusev, Alexander E. Krasnok, Pavel A. Belov, and Yuri S. Kivshar, Resonant Raman scattering from silicon nanoparticles enhanced by magnetic response, Nanoscale **8**, 9721 (2016).
[18] Martín Caldarola, Pablo Albella, Emiliano Cortés, Mohsen Rahmani, Tyler Roschuk, Gustavo Grinblat, Rupert F. Oulton, Andrea V. Bragas, and Stefan A. Maier, Non-plasmonic nanoantennas for surface enhanced spectroscopies with ultra-low heat conversion, Nat. Commun. **6**, 7915 (2015).
[19] E. M. Purcell, Spontaneous emission probabilities at radio frequencies, Phys. Rev. **69**, 681 (1946).
[20] Matthew Pelton, Modified spontaneous emission in nanophotonic structures, Nat. Photonics **9**, 427 (2015).
[21] Sergey I. Bozhevolnyi and Jacob B. Khurgin, Fundamental limitations in spontaneous emission rate of single-photon sources, Optica **3**, 1418 (2016).
[22] Kerry J. Vahala, Optical microcavities, Nature (London) **424**, 839 (2003).
[23] Kasey J. Russell, Tsung-Li Liu, Shanying Cui, and Evelyn L. Hu, Large spontaneous emission enhancement in plasmonic nanocavities, Nat. Photonics **6**, 459 (2012).
[24] Gleb M. Akselrod, Christos Argyropoulos, Thang B. Hoang, Cristian Ciraci, Chao Fang, Jiani Huang, David R. Smith, and Maiken H. Mikkelsen, Probing the mechanisms of large Purcell enhancement in plasmonic nanoantennas, Nat. Photonics **8**, 835 (2014).
[25] Alexander Krasnok, Stanislav Glybovski, Mihail Petrov, Sergey Makarov, Roman Savelev, Pavel Belov, Constantin Simovski, and Yuri Kivshar, Demonstration of the enhanced Purcell factor in all-dielectric structures, Appl. Phys. Lett. **108**, 211105 (2016).
[26] Sergey Makarov, Sergey Kudryashov, Ivan Mukhin, Alexey Mozharov, Valentin Milichko, Alexander Krasnok, and Pavel Belov, Tuning of magnetic optical response in a dielectric nanoparticle by ultrafast photoexcitation of dense electron-hole plasma, Nano Lett. **15**, 6187 (2015).
[27] Maxim R. Shcherbakov, Polina P. Vabishchevich, Alexander S. Shorokhov, Katie E. Chong, Duk-Yong Choi, Isabelle Staude, Andrey E. Miroshnichenko, Dragomir N. Neshev, Andrey A. Fedyanin, and Yuri S. Kivshar, Ultrafast all-optical switching with magnetic resonances in nonlinear dielectric nanostructures, Nano Lett. **15**, 6985 (2015).
[28] Denis G. Baranov, Sergey V. Makarov, Valentin A. Milichko, Sergey I. Kudryashov, Alexander E. Krasnok, and Pavel A. Belov, Nonlinear transient dynamics of photoexcited resonant silicon nanostructures, ACS Photonics **3**, 1546 (2016).
[29] Denis G. Baranov, Sergey V. Makarov, Alexander E. Krasnok, Pavel A. Belov, and Andrea Alù, Tuning of near-and far-field properties of all-dielectric dimer nanoantennas via ultrafast electron-hole plasma photoexcitation, Laser Photonics Rev. **10**, 1009 (2016).

[30] Marco P. Fischer, Christian Schmidt, Emilie Sakat, Johannes Stock, Antonio Samarelli, Jacopo Frigerio, Michele Ortolani, Douglas J. Paul, Giovanni Isella, Alfred Leitenstorfer, Paolo Biagioni, and Daniele Brida, Optical Activation of Germanium Plasmonic Antennas in the Mid-infrared, Phys. Rev. Lett. **117**, 047401 (2016).

[31] Stefano Palomba and Lukas Novotny, Nonlinear Excitation of Surface Plasmon Polaritons by Four-Wave Mixing, Phys. Rev. Lett. **101**, 056802 (2008).

[32] Yongmin Liu, Stefano Palomba, Yongshik Park, Thomas Zentgraf, Xiaobo Yin, and Xiang Zhang, Compact magnetic antennas for directional excitation of surface plasmons, Nano Lett. **12**, 4853 (2012).

[33] J. Lin, J. P. B. Mueller, Q. Wang, G. Yuan, N. Antoniou, X.-C. Yuan, and F. Capasso, Polarization-controlled tunable directional coupling of surface plasmon polaritons, Science **340**, 331 (2013).

[34] Anders Pors, Michael G. Nielsen, Thomas Bernardin, Jean-Claude Weeber, and Sergey I. Bozhevolnyi, Efficient unidirectional polarization-controlled excitation of surface plasmon polaritons, Light Sci. Appl. **3**, e197 (2014).

[35] Yimu Bao, Hao Liang, Huimin Liao, Zhi Li, Chengwei Sun, Jianjun Chen, and Qihuang Gong, Efficient unidirectional launching of surface plasmons by multi-groove structures, Plasmonics **12**, 1425 (2017).

[36] V. S. C. Manga Rao and S. Hughes, Single quantum-dot Purcell factor and β factor in a photonic crystal waveguide, Phys. Rev. B **75**, 205437 (2007).

[37] D. E. Aspnes and A. A. Studna, Dielectric functions and optical parameters of Si, Ge, GaP, GaAs, GaSb, InP, InAs, and InSb from 1.5 to 6.0 eV, Phys. Rev. B **27**, 985 (1983).

[38] A. Femius Koenderink, Plasmon nanoparticle array waveguides for single photon and single plasmon sources, Nano Lett. **9**, 4228 (2009).

[39] A. Alù and N. Engheta, Theory of linear chains of metamaterial/plasmonic particles as sub-diffraction optical nanotransmission lines, Phys. Rev. B **74**, 205436 (2006).

[40] C. F. Bohren and D. R. Huffman, *Absorption and Scattering of Light by Small Particles* (Wiley, New York, 1998).

[41] Roman S. Savelev, Alexey P. Slobozhanyuk, Andrey E. Miroshnichenko, Yuri S. Kivshar, and Pavel A. Belov, Subwavelength waveguides composed of dielectric nanoparticles, Phys. Rev. B **89**, 035435 (2014).

[42] L. Novotny and B. Hecht, *Principles of Nano-Optics* (Cambridge University Press, Cambridge, England, 2006).

[43] P. Yu and M. Cardona, *Fundamentals of Semiconductors* (Springer, New York, 2005).

[44] C. V. Shank, R. Yen, and C. Hirlimann, Time-Resolved Reflectivity Measurements of Femtosecond-Optical-Pulse-Induced Phase Transitions in Silicon, Phys. Rev. Lett. **50**, 454 (1983).

[45] Thibault J. Y. Derrien, Tatiana E. Itina, Rémi Torres, Thierry Sarnet, and Marc Sentis, Possible surface plasmon polariton excitation under femtosecond laser irradiation of silicon, J. Appl. Phys. **114**, 083104 (2013).

[46] See Supplemental Material at http://link.aps.org/supplemental/10.1103/PhysRevApplied.9.014015 for spectral dependences of the Purcell factor for different emitter locations in an orthogonal direction.

[47] Manuel Peter, Andre Hildebrandt, Christian Schlickriede, Kimia Gharib, Thomas Zentgraf, Jens Förstner, and Stefan Linden, Directional emission from dielectric leaky-wave nanoantennas, Nano Lett. **17**, 4178 (2017).

[48] Alexander E. Krasnok, Alex Maloshtan, Dmitry N. Chigrin, Yuri S. Kivshar, and Pavel A. Belov, Enhanced emission extraction and selective excitation of NV centers with all-dielectric nanoantennas, Laser Photonics Rev. **9**, 385 (2015).

[49] Alexander E. Krasnok, Alexey P. Slobozhanyuk, Constantin R. Simovski, Sergei A. Tretyakov, Alexander N. Poddubny, Andrey E. Miroshnichenko, Yuri S. Kivshar, and Pavel A. Belov, An antenna model for the Purcell effect, Sci. Rep. **5**, 12956 (2015).

[50] J. M. Liu, Simple technique for measurements of pulsed Gaussian-beam spot sizes, Opt. Lett. **7**, 196 (1982).

[51] Sergey V. Makarov, Valentin A. Milichko, Ivan S. Mukhin, Ivan I. Shishkin, Dmitry A. Zuev, Alexey M. Mozharov, Alexander E. Krasnok, and Pavel A. Belov, Controllable femtosecond laser-induced dewetting for plasmonic applications, Laser Photonics Rev. **10**, 91 (2016).

[52] Linhan Lin, Jianli Zhang, Xiaolei Peng, Zilong Wu, Anna C. H. Coughlan, Zhangming Mao, Michael A. Bevan, and Yuebing Zheng, Opto-thermophoretic assembly of colloidal matter, Sci. Adv. **3**, e1700458 (2017).

[53] See Supplemental Material at http://link.aps.org/supplemental/10.1103/PhysRevApplied.9.014015 for the nanoantenna design based on cylindrical Si particles.

[54] D. H. Reitze, T. R. Zhang, W. M. Wood, and M. C. Downer, Two-photon spectroscopy of silicon using femtosecond pulses at above-gap frequencies, J. Opt. Soc. Am. B **7**, 84 (1990).

[55] G. A. Wurtz, R. Pollard, W. Hendren, G. P. Wiederrecht, D. J. Gosztola, V. A. Podolskiy, and A. V. Zayats, Designed ultrafast optical nonlinearity in a plasmonic nanorod metamaterial enhanced by nonlocality, Nat. Nanotechnol. **6**, 107 (2011).

[56] Ventsislav K. Valev *et al.*, Plasmon-enhanced sub-wavelength laser ablation: Plasmonic nanojets, Adv. Mater. **24**, OP29 (2012).

[57] Dmitry A. Zuev, Sergey V. Makarov, Ivan S. Mukhin, Valentin A. Milichko, Sergey V. Starikov, Ivan A. Morozov, Ivan I. Shishkin, Alexander E. Krasnok, and Pavel A. Belov, Fabrication of hybrid nanostructures via nanoscale laser-induced reshaping for advanced light manipulation, Adv. Mater. **28**, 3087 (2016).

[58] Yuanmu Yang, Wenyi Wang, Abdelaziz Boulesbaa, Ivan I. Kravchenko, Dayrl P. Briggs, Alexander Puretzky, David Geohegan, and Jason Valentine, Nonlinear Fano-resonant dielectric metasurfaces, Nano Lett. **15**, 7388 (2015).